

Interaction of Laser Beam with PZT – Target and Observation of Laser – Induced Plume and Particle Ejection

B. W. Lee

Laser와 PZT – Target간의 반응과 그에 따른 Plume 형성 및 입자 방출에 관한 연구

이 병 우

Key words : KrF excimer laser, PZT – target, Laser – target interaction, Laser – induced plume(plasma), Pulsed laser deposition, Optical diagnostics, Particle ejection

Abstract

Laser – induced plume and laser – target interaction during pulsed laser deposition are demonstrated for a lead zirconate titanate (PZT). A KrF excimer laser (wavelength 248nm) was used and the laser was pulsed at 20Hz, with nominal pulse width of 20ns. The laser fluence was $\sim 16\text{J}/\text{cm}^2$, with 100mJ per pulse. The laser – induced plasma plume for nanosecond laser irradiation on PZT target has been investigated by optical emission spectra using an optical multichannel analyzer(OMA) and by direct observation of the plume using an ICCD high speed photography. OMA analysis showed two distinct ionic species with different expansion velocities of fast or slow according to their ionization states. The ion velocity of the front surface of the developing plume was about $10^7\text{cm}/\text{sec}$ and corresponding kinetic energy was about 100eV. ICCD photograph showed another kind of even slower moving particles ejected from the target. These particles considered expelled molten parts of the target. SEM morphologies of the laser irradiated targets showed drastic melting and material removal by the laser pulse, and also showed the evidence of the molten particle ejection. The physics of the plasma(plume) formation and particle ejection has been discussed.

Introduction

Pulsed laser has been used for drilling, welding, and cutting a variety of materials. Recently, pulsed laser deposition (PLD) with use of excimer laser is becoming the method of choice for the preparation of multicomponent materials in thin film forms. PLD process has gained considerable attention with regard to the preparation of high T_C superconducting thin films^{1,2}. Many other types of materials have been successfully deposited using PLD; these include metals, biomaterials, and ferroelectrics^{3,4,5}. The intensity of research in ferroelectric thin films has been driven primarily by their attractiveness for use in non-volatile random access memory (RAM) devices⁶. One material, in particular, $PbZr_xTi_{1-x}O_3$ (PZT), shows great promise for this application because of its intrinsically high remanent polarization and dielectric strength. Laser-based systems offer a number of advantages⁷ for film deposition. Virtually any solid material can be used as a target, including those with complex multicomponent compositions. Similarly, there is no inherent limitation on the substrate material, and films can be deposited under a variety of conditions, including the presence of active gases, or the use of heated substrates. Another promising characteristic of the laser deposition is little difference in the composition between the target material and the deposited film.

The film growth process from PLD is, in general, a complex convolution of several processes: material ejection from the laser-target interaction, chemical and physical interactions of the evaporated material with gas ambient, and finally surface interactions on the substrate.

In this study, the laser-target interaction is

focused. The use of optical diagnostics as a tool in studying the complex chemical interactions occurring in the vapor plume will be demonstrated. The vapor plumes produced by laser-induced vaporization have practical application as a material transport medium for the deposition of ceramic thin films. The physical interactions occurring during laser-induced mass transport are complex, and include melting, vaporization, particle ejection, ion etching, and plasma condensation. Most film deposition methods utilize pulsed, rather than continuous wave excitation, as this produces larger instantaneous power output without raising the temperature of the bulk target significantly. Time-dependent phenomena are important during laser irradiation. The material exiting the surface during initial plume generation may interact further with the tail of the incoming laser pulse. The laser-generated plume typically has a strong directional component, and the resulting optical spectra are very complex, with contributions from ions as well as neutrals which vary both temporally and spatially.

Several imaging experiments of the laser-target interaction have been also conducted^{8,9}, but the researchers could not separate the particle ejection from the glowing plasma plume. This study has shown a separation of the bright plasma (plume) and particles. It is the intention to present new observations which provide additional support for the general utility of the laser method as a means for producing very fine-grained films of ceramic material, as well as films containing a mixture of particles of different sizes. Although the presence of both a relatively coarse and a relatively fine-grained component (particle) in laser-generated deposits has been noted in the literature¹⁰, the fact that extremely fine-grained films of

multicomponent bulk compositions can be produced which are homogeneous both physically and chemically on a scale of a few nanometers may not be widely realized. These attributes appear to be related to the direct condensation of material from the vapor plume.

Experimental

Laser Deposition Facility

The laser deposition facility consists of a high power pulsed laser system, deposition chamber, and ancillary analysis equipment. The laser used in this work was a KrF excimer laser (wavelength 248nm). The laser was pulsed at 20Hz, with nominal pulse width of 20ns. Fluence was $\sim 16\text{J}/\text{cm}^2$, with 100mJ per pulse. A radiometer was used to directly measure the laser energy. These measurements were made periodically during experimental runs to confirm constant laser power conditions. Deposition took place in an evacuated chamber, with a background oxygen pressure of 13.33Pa.

The cylindrical deposition chamber was constructed of stainless steel and had internal dimensions of 20cm in diameter and 8cm high. The chamber was equipped with multiple ports for: mounting targets and substrates, laser access to the targets, and optical imaging and spectroscopic observations of the laser generated plumes. The reaction chamber was continuously evacuated to 10mPa by a roughing pump-backed diffusion pump. The laser beam was brought into the chamber and focused onto the target at an incidence angle of 35° using a 20cm focal length lens through a windowed vacuum port. The background oxygen gas pressure in the deposition chamber was introduced through a needle valve from a ballast tank whose pressure was servo controlled to obtain

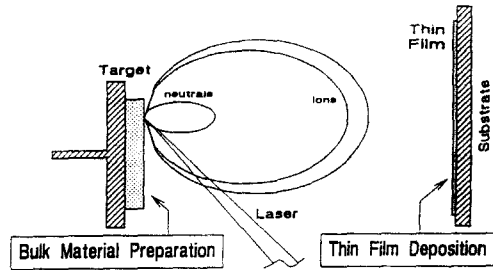


Fig. 1 Schematic configuration of KrF pulsed laser deposition.

the desired background pressure. Side ports on the chamber allowed for several line-of-sight optical access paths perpendicular to the laser-plume axis. Other side ports on the chamber were available for electrical probing of the plume ions and optical probing of the plume particulates.

The geometry of the deposition system is shown in Fig. 1. During deposition, a luminous plume was produced, the axis of which was perpendicular to the target surface. Since the pulse duration of the laser was short compared to the pulse rate, the sample cooled nearly to the ambient temperature between laser shots.

Optical Diagnostics

An optical multichannel analyzer (OMA), consisting of a 0.275 meter monochromator with a gateable intensified photodiode array, was used to record the emission spectra synchronous with the laser. An intensified charge-coupled device (ICCD) array photography is used to observe the glowing plume expansion and detect the particles ejected from the target. The timing of the laser firing, OMA gate and ICCD array were controlled by a laboratory computer. The computer was used to plot the data from OMA and the ICCD images. A fused silica 10cm focal length lens was used at twice its focal length to obtain one-to-one imaging of the plume on the entrance slit of the OMA and

ICCD array.

Materials and Materials Characterization

Targets were dense stoichiometric ceramic, diameter of ~ 2.5 cm. The targets of $\text{PbZr}_{0.53}\text{Ti}_{0.47}\text{O}_3$ (PZT) composition were prepared by conventional oxide sintering method at 1250°C and their phase chemistry was verified by powder x-ray diffraction.

Typical grain size examined by a scanning electron microscope(SEM) was $3\sim 5\mu\text{m}$. During typical experiments, the focused laser beam irradiated a large number of grains during any given pulse. The targets were fixed or rotated. Single and multiple laser shots were irradiated on a different area of the fixed target and a crater structure was formed. The rotating target was continuously translated back and forth along one direction, so that each shots focused on a different area of the target and the target was uniformly removed.

Substrates were silicon single crystal wafer which were coated with 200nm platinum. The substrate were mounted in the deposition chamber by a stationary substrate holder. The target to substrate distance was 3.0cm.

Results and Discussion

A theoretical description of laser-solid interaction is complex and draws from many disciplines. The dominant laser-target interaction mechanism depends on the laser pulse width(duration), power density, wavelength and the target itself¹¹⁾. For low power(e.g. $< 3\text{J}/\text{cm}^2$) and long pulse width(e.g. $> 100\mu\text{s}$) melting will dominate which is favorable for welding. As the power density increases ($> 3\text{J}/\text{cm}^2$) or the pulse width decreases, vaporization dominates; in this study, power

density(fluence) was high as $16\text{J}/\text{cm}^2$ and pulse width was short as 20ns as mentioned. For this high power density and short pulse width, the vaporization dominates and the evaporation from the target is stoichiometric without compositional segregation which is due to the anisotropic absorption of the surface for the case of low power density and long pulse width. In PLD process, the model which can be developed by the absorption of the incident laser beam is classified as follows: (1) the interaction of the laser beam with the target, (2) generation and expansion of laser induced plume towards the substrate, (3) plume condensation on the surface of substrate, leading to deposition of thin films, (4) possible additional processes (e.g. plasma etching and particle ejection). The interaction of nanosecond high-power laser beams with the bulk target leads to very high surface temperatures(typically $> 2000^\circ\text{C}$), which results in emission of positive ions and electrons. The thermionic emission of positive ions can be calculated by the Langmuir-Saha equation¹²⁾. This equation is expressed as

$$i_+/i_0 = (g_+/g_0)\exp[(\Phi - I)/KT],$$

where i_+ and i_0 are, respectively, positive and neutral ion fluxes leaving the surface at temperature T , g_+ and g_0 are, respectively, the statistical weight of ionic and neutral states, Φ is the electron work function, K is the Boltzmann's constant, and I is the ionization potential of the material departing from the surface. Since $I > \Phi$, the fraction of ionized species increases with increasing temperature. As a result of this process, an appreciable flux of positive ions and electrons is produced during the PLD. A brilliant glow of laser plasma, plume, is produced and extending outward from the surface.

Spectral Analysis and Direct Observation of the Plume

Time resolved emission spectra of the plume can be obtained by using a 10ns gate on the OMA and aperturing the entrance slit of the OMA's monochromator as described before. Fig. 2 shows the time - resolved emission spectra from the laser - induced plume 10mm above a PZT target irradiated by the focused laser beam. Spectral features attributed to doubly and triply ionized Ti and Zr, and singly ionized Pb appear at the early stage of the laser - surface interaction (< 200ns). The dominant spectral features which appears at later times are due to slower - moving, singly - ionized Zr, Ti, and neutrals. Identification of time - resolved spectral features is aided by analysis of plume emission from Ti, Zr, and Pb pure targets. Electrons being much lighter than ions expand rapidly and generate electric field at the front of plasma surface. Ions are accelerated by this field. Therefore, species with higher states of ionization have greater velocities as a result of the field. The ion velocity of the front surface of the developing plume is about

10⁷cm/sec. The velocity and those of the other ionic species present correspond to kinetic energies of from 50 to 100eV. These high kinetic energies of the ionic species in the deposition process are likely to be very important in the formation of gas phase products (in this case, forming oxides with ambient oxygen gas) that deposit on the substrate and also help the crystallization of the films at relatively low substrate temperature compared with those of other deposition methods because of improved surface diffusion and mobility of the ions.

Fig. 3 shows computer plotted ICCD images of the expansion trajectory of PZT plasma from the target. The observable bright glow of the plume begins to appear about 200ns after the start of the laser pulse (pulse width, 20ns), and the plume expands and fades relatively slowly thereafter which lasts for ~10 μ s. The delay of the emission pulse with respect to the laser pulse is of interest in elucidating the processes occurring. This is assumed as follows: there is a rapid heat absorption at the target surface, which can produce the transient vaporization and ionization of the surface. The transiently

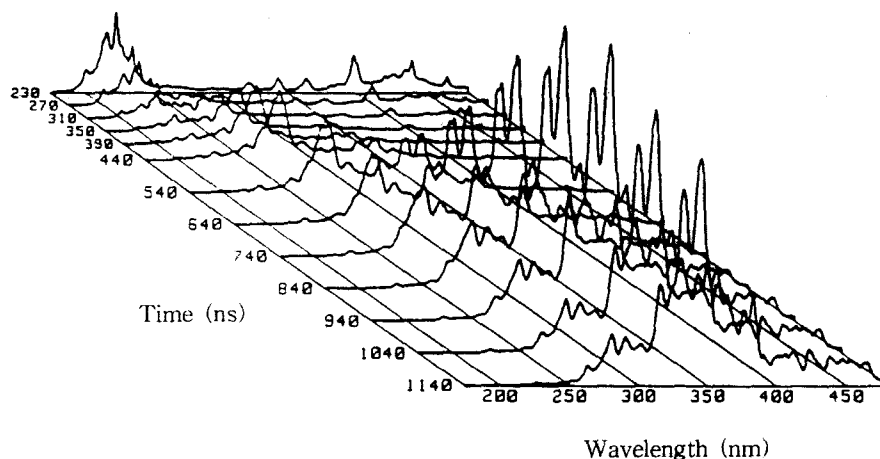


Fig. 2 Time - resolved optical emission spectra of the laser generated plume from a PZT target from 10mm above the surface. The laser was on at 200ns.

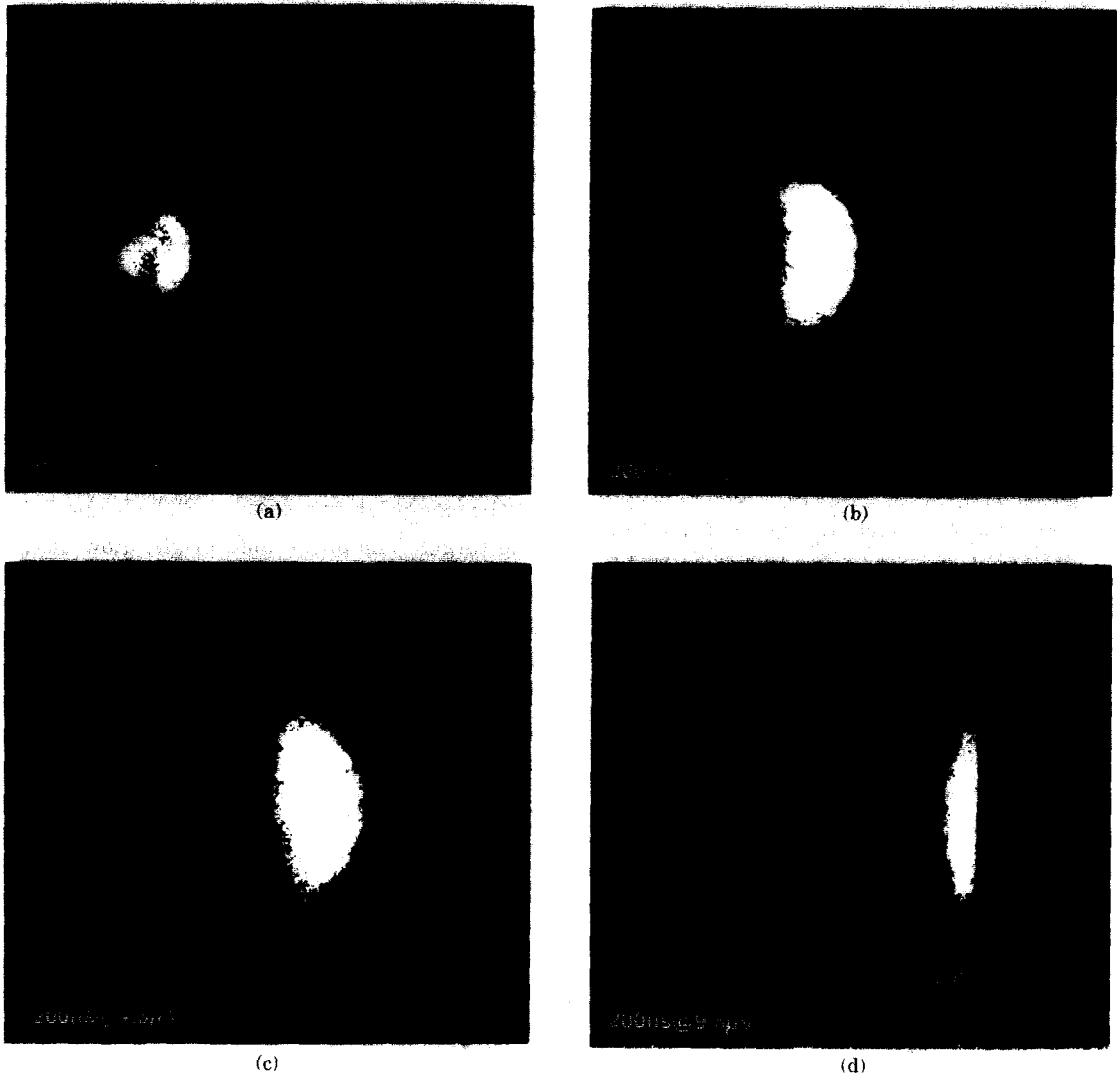


Fig. 3 Computer plotted ICCD images tracing the glowing plasma(plume) expansion. Exposure was 200ns and time delays were as follows : (a) 500ns, (b) 1.5µs, (c) 4.5µs, (d) 9.5µs.

vaporized surface may become cooler than the sub-surface regions because of evaporation. This non-equilibrium situation leads to a pulse of high pressure and subsequent superheating of the underlying material until the temperature rises above the critical point. There is no longer any distinction between the superheated solid and the highly condensed gas. The emission of the vaporized material,

which is delayed relatively to the peak of the temperature pulse at the surface, proceeds like a thermal explosion. This explosive evaporation is also presumed cause of the highly forward directed plume(note the laser incidence angle which was 35°).

ICCD images from the PZT target clearly showed a separation of the bright plasma which lasted $\sim 10\mu\text{s}$ and particles which begins

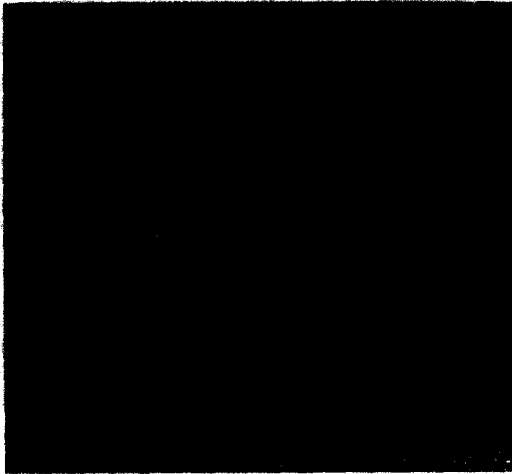


Fig. 4 Computer plotted ICCD image of the glowing particles ejected from the target.
Exposure was 50 μ s and time delay was 500 μ s.

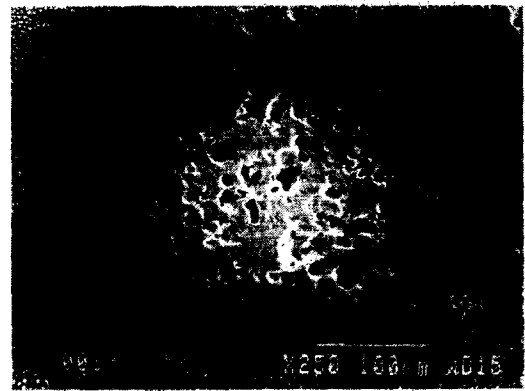
to appear $\sim 270\mu$ s after the laser pulse. Fig. 4 shows the computer generated ICCD photograph taken at 500 μ s after the laser pulse with exposure of 50 μ s. The photograph shows many bright spots and the spots mean still very hot and much slower moving particles ejected from the target toward the substrate. These particles considered expelled molten parts of the target. It is not clear how these particles are produced. Regarding the ejection of the particles found in some metal and ceramic films, several models^{13,14,15} have been proposed. Among them, one possibility is a shock wave model¹⁵. The rapid surface evaporation and consequent recoil pressure could cause the generation of shock wave at the target surface. The shock wave could result in the splashing (ejection) of the liquid layer underneath the evaporation front.

Laser Induced Morphology of PZT - Target

An examination of the PZT target itself will give some insights into the plume generation and particle ejection. To make flat target sur-



(a)



(b)

Fig. 5 SEM photographs of the laser irradiated PZT - target : (a) after one pulse, (b) after 10 pulses.

face and to observe the laser irradiation effect easily, the PZT as - prepared was abraded with # 2000 SiC paper and polished with 0.05 μ m alumina abrasive powders. Fig. 5 shows SEM micrographs of fixed PZT target after being irradiated with laser shots (20ns, 248 μ m). After one laser pulse (Fig. 5(a)), the rounded appearance of the surface is shown in the target. The morphology suggests melting, but probably only in a very thin layer, as there appears to be no tendency for pooling of the liquid or filling of voids. Thus the liquid film is probably removed in this process by vaporization as rapidly as melting takes place. The

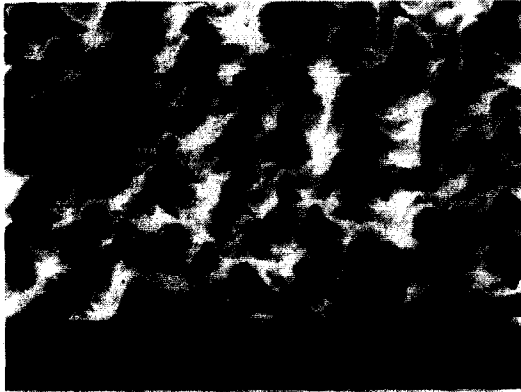


Fig. 6 SEM photograph of the rotated and translated PZT -target. The target was uniformly irradiated for 30min.

grain boundaries removed at the beginning by the abrasion are also shown in the micrograph, which indicates that there was an etching by the reaction of reactive chemical species of plasma with the target surface. After 10 laser pulses (Fig. 5(b)), a crater structure is formed and many deep holes are found in the center of irradiated area as materials were removed from the target. The holes present that the material removal was explosive fashion which was expected. Evidence for melting and recoil pressure is clear from such features as congealed liquid stream of viscous flow and small droplet formation on the top of the ridge which appear at the surrounding edge: the droplets may represent molten or partially molten viscous flow which was frozen with inadequate escape velocities. Fig. 6 shows a SEM micrograph of the rotated and translated target which was irradiated uniformly for 30min. A conical structure is formed as material was removed from the target and the congealed droplets are also shown on the top of the cone. The morphology is an evidence of obvious melting and (large) particle ejection (note the necking of some droplets and their size of $\sim 1\mu\text{m}$), with the effect resembling a frozen liquid



Fig. 7 SEM photograph of a typical PZT film.

splash pattern. Also, materials removed from the small holes shown in the trench are likely responsible in the (small) particle deposition (note the submicron hole size). Fig. 7 shows a representative SEM micrograph of an as-deposited thin film. The film is composed of extremely fine grained ($< 10\text{nm}$) base film and spherical particles ranging from submicron to a micron size. Spherical shape of the particles suggest that they have been molten state during deposition. The spherical particles are believed to be caused by the ejection of melted target material. The experiments have confirmed that the film formed by the PLD process consist of three components: (1) a relatively coarse fraction in the range of $\sim 1.0\mu\text{m}$ and (2) a rather fine fraction in the range of submicron ($\sim 0.2\mu\text{m}$); both the components are believed to have been physically ejected molten particles from the droplets and trench of the target, respectively, as described above, and (3) the extremely fine grained fraction having a smooth morphology as a base film formed by condensed vapor from the plume.

Conclusion

In conclusion, the dynamics of the laser depo-

sition process of PZT has been investigated by optical measurements. The standard picture of material removal by high power density laser beam from a solid surface assumes many step processes. As the laser beam hits the target, photons are absorbed by the surface, forming a molten layer that vaporizes. The vaporization process creates a surface cooling and/or a kind of recoil pressure on the liquid layer and again vaporizes or expels the molten material.

Study of the optical spectra of plume showed that the species with higher states of doubly and triply ionized appeared at the early stage of the laser - surface interaction and had higher expansion velocities than those of singly ionized species or neutrals which appeared at later times. ICCD photography showed much slower moving particles. These particles considered expelled molten parts of the target. The mechanism of the particle ejection has been proposed by the recoil pressure resulting from rapid surface evaporation and consequent shock wave, which leads to the splashing of the molten part of the target.

The results confirm the existence of three - defined particle size distributions in most film deposits : a coarser ($\sim 1.0\mu\text{m}$) and a rather finer ($\sim 0.2\mu\text{m}$) fraction physically ejected from the target surface but having different origins, while the finest fraction ($< 10\text{nm}$) may arise from vapor(plume) condensation.

The present work will provide fundamental insight of laser - target interaction and information useful in controlling precisely the film morphology.

References

- 1) S. Witanaichi, H. S. Kwok, X. W. Wang, and D. T. Shaw, "Deposition of Superconducting Y - Ba - Cu - O Films at 400°C without Post - annealing," *Appl. Phys. Lett.*, Vol. 53, No. 3, 234 - 236, 1988.
- 2) D. B. Chrisey and A. Inam, "Pulsed Laser Deposition of High T_c Superconducting Thin Films for Electronic Device Applications," *MRS Bull.*, Vol. XVII, No. 2, 37 - 43, 1992.
- 3) S. R. Nishitani, S. Yoshimura, and M. Yamaguchi, "Deposition of Nitrides and Oxides of Aluminum and Titanium by Pulsed Laser Irradiation," *J. Mater. Res.*, Vol. 7, No. 3, 725 - 733, 1992.
- 4) T. Venkatesan, X. D. Wu, R. Muenchausen, and A. Pique, "Pulsed Laser Deposition : Future Directions," *MRS Bull.*, Vol. XVII, No. 2, 54 - 58, 1992.
- 5) M. G. Norton, K. P. B. Cracknell, and C. B. Carter, "Pulsed - Laser Deposition of Barium Titanate Thin Films," *J. Am. Ceram. Soc.*, Vol. 75, No. 7, 1999 - 2002, 1992.
- 6) S. K. Dey, "Integrated Pb - perovskite Dielectrics For Science and Technology," *Ferroelectrics*, Vol. 135, 117 - 130, 1992.
- 7) H. Kidoh and T. Ogawa, "Ferroelectric Properties of Lead - Zirconate - Titanate Films Prepared by Laser Ablation," *Appl. Phys. Lett.*, Vol. 58, No. 25, 2910 - 2912, 1991.
- 8) F. P. Gagliano and U. C. Paek, "Observation of Laser - Induced Explosion of Solid Materials and Correlation with Theory." *Applied Optics*, Vol. 13, No. 2, 274 - 279, 1974.
- 9) O. Eryu, K. Murakami, and K. Masuda, "Dynamics of Laser - ablated Particles from High T_c Superconductor $\text{YBa}_2\text{Cu}_3\text{O}_y$," *Appl. Phys. Lett.*, Vol. 54, No. 26, 2716 - 2718, 1989.
- 10) T. Venkatesan, X. D. Wu, A. Inam, and J. B. Wachtman, "Observation of Two Distinct Components During Pulsed Laser Deposition of High T_c Superconducting Films", *Appl. Phys. Lett.*, Vol. 52, No. 14, 1193 - 1195, 1988.
- 11) S. Otsubo, T. Maeda, T. Minamikawa, Y. Yonezawa, A. Morimoto, and T. Shimizu, "Preparation of $\text{Pb}(\text{Zr}_{0.52}\text{Ti}_{0.48})\text{O}_3$ Films by Laser Ablation," *Jpn. J. Appl. Phys.*, Vol. 29, No. 1, L133 - L136, 1990.
- 12) R. K. Singh, O. W. Holland, and J. Narayan,

- "Theoretical Model for Deposition of Superconducting Thin Films Using Pulsed Laser Evaporation Technique," *J. Appl. Phys.*, Vol. 68, No. 1, 2233 - 2247, 1990.
- 13) J. F. Ready, "Development of Plume of Material Vaporized by Giant Pulse Laser, *Appl. Phys. Lett.*, Vol. 3, No. 1, 11 - 13, 1963.
- 14) R. Kelly, J. J. Cuomo, P. A. Leary, J. E. Rothenberg, B. E. Braren, and C. F. Aliotta, "Laser Sputtering: Part I," *Nucl. Instr. and Meth.*, B9, 329 - 340, 1985.
- 15) R. A. Olstad and D. R. Olander, "Evaporation of Solids by Laser Pulses. I. Iron", *J. Appl. Phys.*, Vol. 46, No. 4, 1499 - 1508, 1975.